THE JOURNAL OF PHYSICAL CHEMISTRY A
A JOURNAL OF THE AMERICAN CHEMICAL SOCIETY

pubs.acs.org/JPCA

Article

Measuring Photodissociation Product Quantum Yields Using Chemical Ionization Mass Spectrometry: A Case Study with Ketones

Michael F. Link,* Delphine K. Farmer, Tyson Berg, Frank Flocke, and A. R. Ravishankara*

Cite This: *J. Phys. Chem. A* 2021, 125, 6836–6844

Read Online

ACCESS | Metrics & More | Article Recommendations | Supporting Information

ABSTRACT: Measurements of photolysis quantum yields are challenging because of the difficulties in measuring the first-generation photodissociation products, interference from other products or contaminants, sufficient photon fluxes and/or low absorption cross sections of the photolyte to make detectable amounts of products, and quantification of the photon flux. In the case of acetone (and other atmospherically relevant ketones) the uncertainty in the photolysis quantum yield creates uncertainty in the calculated OH radical and acyl peroxy nitrate production in the atmosphere. We present a new method for determining photodissociation product quantum yields by measuring acyl peroxy radicals ($RC(O)O_2$) produced in the photolysis of ketones in air using chemical ionization mass spectrometry (CIMS). We show good agreement of our CIMS method with previously published quantum yields of the acyl radical from photolysis of biacetyl and methyl ethyl ketone (MEK) at 254 nm. Additionally, we highlight the capabilities of this CIMS method through the measurement of photolysis branching ratios for MEK. We suggest future applications of CIMS (in the laboratory and field) to measure $RC(O)O_2$ and associated photolysis processes.

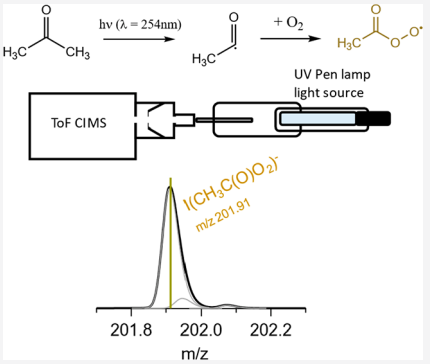

INTRODUCTION

Measurement of photodissociation quantum yields is challenging because of the inability to produce measurable concentrations of direct photodissociation products (due to low absorption cross sections of the photolyte and/or the available photon flux), multiple product formations, interference by numerous post-photon-absorption reactions, and the quantification of the photon flux or fluence. Therefore, various methods that rely on end-product analyses,[1,2] proxies for photodissociation products,[3] and relative yield measurements[4] have been utilized. The quantum yield measurements for acetone exemplify these issues. Numerous methods have yielded differing results for the formation of the acetyl radical ($CH_3C(O)$) from acetone photolysis, with the largest discrepancies occurring at the atmospherically relevant wavelengths above 300 nm.[2,3,5,6]

Ketones are primarily important in the chemistry of the troposphere for two reasons: (1) They can be sources of OH and HO_2 radicals[7−9] where water concentrations are very low (e.g., in the upper troposphere, where the estimated contribution is as high as 95% from this source[9]); and (2) they are ready-made sources for acyl peroxy radicals ($RC(O)O_2$), which make peroxyacyl nitrates that transport NO_x ($NO + NO_2$) over long distances.[10] Yet, there are significant uncertainties in the quantum yields of products in ketone photolysis.[11]

Most previous studies of ketone photolysis used end-product analysis or indirect methods to quantify photodissociation product quantum yields.[12−14] Even in the case of acetone (the simplest ketone) there are conflicting reports of photodissociation quantum yields based on measurements of the loss of acetone, measurements of products such as CO,[2,5] Br formed from the reaction of acyl or methyl radical with Br_2,[4] and OH as a proxy for $CH_3C(O)$ via its reaction with O_2 that generates OH.[6,15] The $CH_3C(O)$ radical from ketone photolysis has only been detected via its visible absorption using cavity ringdown spectroscopy.[16] The visible absorption of $CH_3C(O)$ is continuous, and it would be hard to separate the absorptions by $CH_3C(O)$ from those of similar radicals, for example, the propanoyl acyl radical ($CH_3CH_2C(O)$) that is produced in the photolysis of another atmospherically relevant ketone, methyl ethyl ketone (MEK). In this study, we target the measurement of $RC(O)O_2$ as they are the major intermediates formed from the reaction of primary ketone photodissociation products in air, representing atmospherically relevant quantum yields. The NASA/JPL evaluations of kinetics and photochemical data describe the current state our understanding.[11]

Received: April 7, 2021
Revised: July 11, 2021
Published: July 29, 2021

https://doi.org/10.1021/acs.jpca.1c03140
J. Phys. Chem. A 2021, 125, 6836−6844

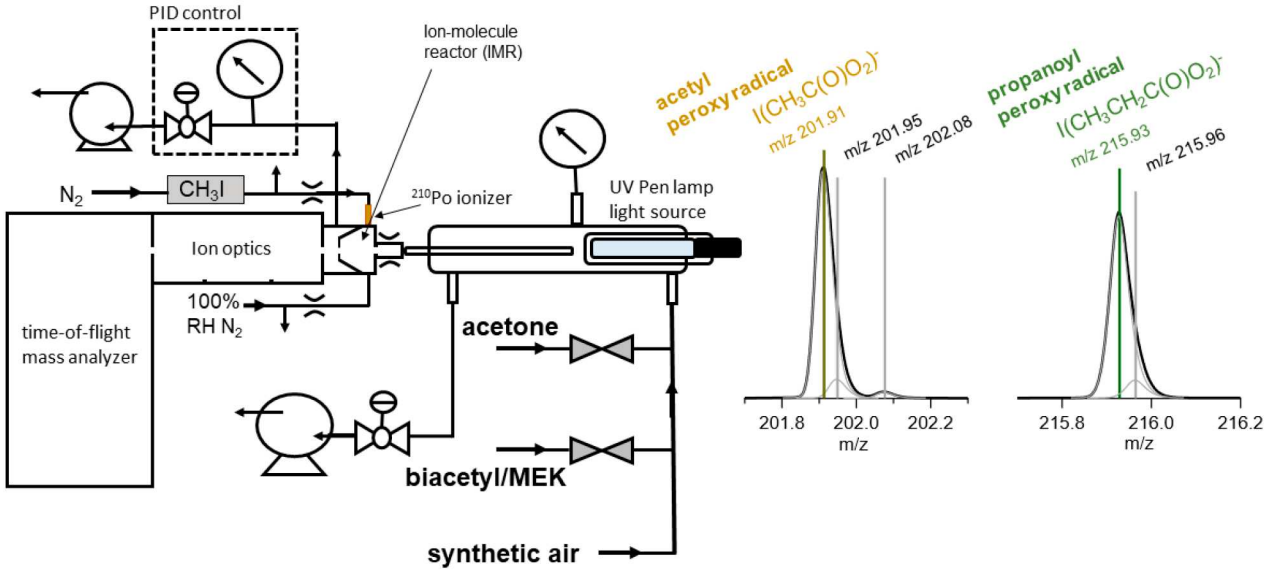

Figure 1. Schematic of the experimental layout (left) with the high-resolution mass spectrum used to detect $CH_3C(O)O_2$ and $CH_3CH_2C(O)O_2$ on the right. The ability to distinguish between the mass of interest from the signal due to background species is shown in the mass spectra. The limit of detection for $CH_3C(O)O_2$ (1 s averaging) in our system was 6 ppt_v (~1.3×10^8 cm^{-3} at 865 mbar).

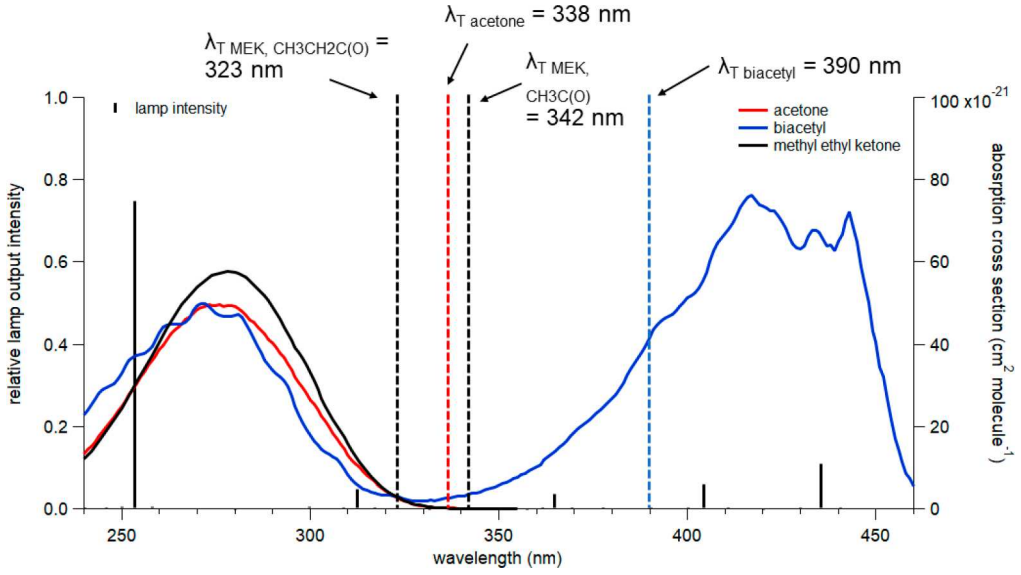

Figure 2. Relative UV Pen-Ray lamp (Analytik Jena, PN 90-0012-02) output (left axis), provided by the vendor, as a function of wavelength (black vertical bars). Various mercury lines are visible. The intensities of these lines could vary a little depending on the condition of the lamp. The absorption cross sections for all three ketones in this study (right axis) are also plotted as a function of wavelength. Acetone and MEK cross sections are from NASA/JPL[11] and that for biacetyl is from IUPAC.[21] Both acetone and MEK have negligible absorption at lamp wavelengths beyond 340 nm. However, biacetyl has a second absorption band that overlaps the longer wavelength emission lines. Threshold photolysis wavelengths (λ_T) shown in the figure are calculated from standard enthalpies of formation at 298 K given in NASA/JPL evaluations.[11] The energy threshold for the photodissociation of biacetyl to give $CH_3C(O)$ radicals is 390 nm. Therefore, absorption of the 405 and 436 nm lines should contribute negligibly to the measured $CH_3C(O)$ quantum yield.

IODIDE CHEMICAL IONIZATION MASS SPECTROMETRY (CIMS) MEASUREMENT OF PEROXY RADICALS ($RC(O)O_2$)

We used CIMS to measure $RC(O)O_2$ produced in air from the photolysis of three important atmospheric ketones (acetone, biacetyl, and MEK) and measured quantum yields at 254 nm for the production of the RC(O) radical. We used a high-resolution time-of-flight chemical ionization mass spectrometer (ToF-CIMS)[17] equipped with an iodide ion source[18−20] (Aerodyne Research Inc., Billerica, MA). We detected and quantified $RC(O)O_2$ produced from ketone photolysis, in air, as iodide−analyte adducts (Figure 1). Use of ToF-CIMS allows us to not only distinguish between $RC(O)O_2$ species (e.g., $CH_3C(O)O_2$ and $CH_3CH_2C(O)O_2$) but also distinguish the product of interest from background contributions at very nearly the same mass. For example, we operated at high resolution (4100 at m/z 202) to differentiate between multiple peaks at the same nominal mass as seen in the mass spectrum

https://doi.org/10.1021/acs.jpca.1c03140
J. Phys. Chem. A 2021, 125, 6836−6844

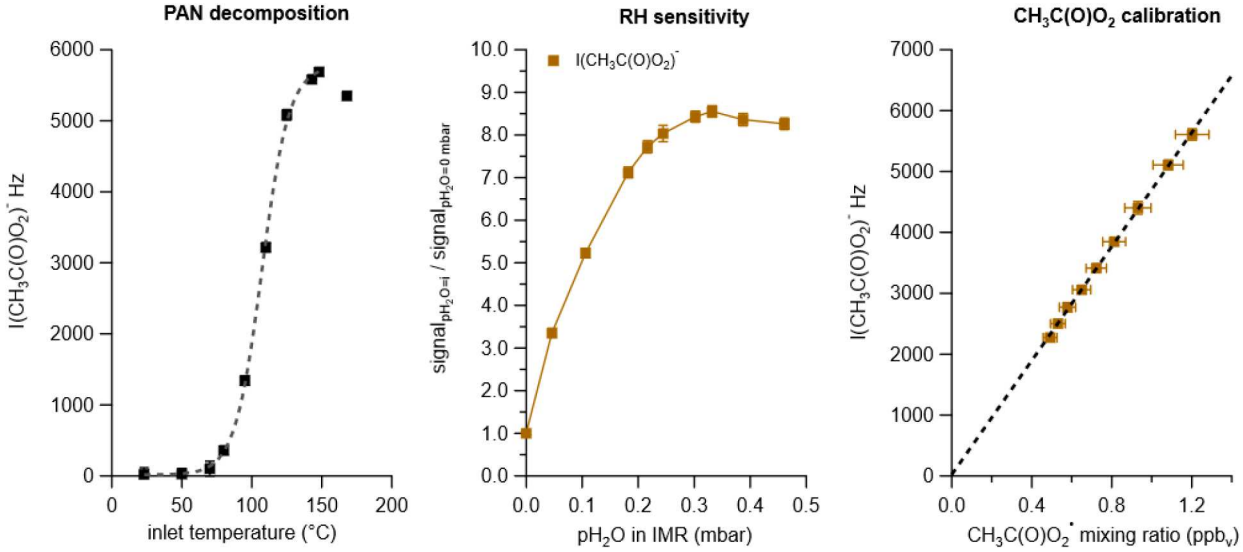

Figure 3. Peroxy acetyl nitrate (PAN) (40 ppb_v) was generated from a home-built source, diluted in the flow, and thermally dissociated to form $CH_3C(O)O_2$ for detection by the ToF-CIMS. The optimal PAN decomposition to $CH_3C(O)O_2$ was obtained with a ToF-CIMS calibration inlet temperature of 150 °C (left panel). The formation of the $I(CH_3C(O)O_2)^-$ ion was dependent on water vapor concentration in the IMR with signal maximizing at water partial pressures (pH_2O) in the IMR of >0.3 mbar (middle panel), after which it was roughly constant. The calibration of the $I(CH_3C(O)O_2)^-$ ion was performed at ∼0.5 mbar pH_2O in the IMR (right panel). The LOD for $CH_3C(O)O_2$ (1 s averaging) in our system was 6 ppt_v.

for $I(CH_3C(O)O_2)^-$ at m/z = 202 (Figure 1). Only one of them at m/z = 201.91 is the ion of interest.

Absorption of light by the ketone leads to an excited molecule, which can undergo different processes[14] and yield dissociation products (e.g., acyl radicals, alkyl radicals, CO, and alkanes) or be quenched back to states that cannot dissociate (ultimately to the ground state in multiple steps). Here we focus only on the production of the acyl peroxy radicals in the photolysis of the ketones in air to show that our method works; i.e., it is a proof of concept.

Figure 1 shows the layout of our experiment and the quality of mass spectral data that was obtained. A 1 in. O.D. Pyrex tube was used as the photolysis-reaction chamber in which a smaller 0.5 in. O.D. quartz test tube was inserted to house a UV Pen-Ray lamp ("ozone-free"). The use of the quartz allows 254 nm light into the reactor. The temperature in the housing for the lamp was ∼30 °C when the lamp was lit as measured by a thermocouple inserted into the housing. The emissions from the Pen-Ray lamp used for this study are shown in Figure 2.

This lamp photolyzed a flowing mixture of ultrahigh purity (UHP) nitrogen and oxygen (∼21% O_2) containing known concentrations of acetone, MEK, or biacetyl. A volumetric flow of 7 L per minute was maintained in the reactor during all photolysis experiments. Mixtures of ketones were prepared in UHP N_2 in 12 L Pyrex bulbs by diluting gaseous ketones from the headspaces of degassed liquid ketones. They were introduced to the bath gas flow controlled by two-way solenoid valves. The ketone concentrations in the bulbs were measured via absorption of 254 nm light (from a mercury lamp) in a separate cell. The precision (twice the standard deviation of the mean) of the measured ketone concentrations in the bulb was better than ±5%. A 0.25 in. O.D. Pyrex tube connected the ion−molecule reactor (IMR) of the ToF-CIMS directly to the photolysis flow cell and was inserted into the flow cell to sample from the center of the flow. We controlled the reactor's pressure in the range of 90−865 mbar using a needle valve and a scroll pump in line with the reactor. Additionally, we maintained the pressure of the IMR at 65 mbar. The residence time between the photolysis region and sampling inlet was minimized (∼0.3 s) to reduce the influence of secondary reactions.

The contents of the photolysis reactor were sampled into the IMR. Iodide ions were supplied to the IMR by flowing methyl iodide (from a heated permeation source) in UHP N_2 through a ^{210}Po ionizer. The IMR of the ToF-CIMS was operated with a constant concentration of water vapor (around 0.5 mbar, which could not be exceeded due to the saturation vapor pressure) to keep the formation efficiency of iodide adducts constant (Figure 3). The formation efficiency can change through ligand-exchange reactions.[18]

$CH_3C(O)O_2$ and $CH_3CH_2C(O)O_2$ were detected as iodide adducts (gray peaks in Figure 1 represent unidentified background signals). Known concentrations of $CH_3C(O)O_2$ were generated by thermally dissociating known concentrations of peroxy acetyl nitrate, PAN (Figure 3), from a home-built source.[22] Details of the $CH_3C(O)O_2$ calibration experimental setup (Figure S1) are presented in the Supporting Information. The obtained plot of the ion intensity with the radical concentration is linear (r^2 = 0.998). The slope shows that we can detect very small concentrations of the radical (4.68 ± 0.05 Hz ppt_v^{-1}) with a limit of detection[17] (LOD) of 6 pptv (for 1 s averaging time). The noted LOD accounts for not only the noise but also the background level, B, via the equation

$$\frac{S}{N} = \frac{\text{Sensitivity}_{RO2}[RO_2]t}{\sqrt{\text{Sensitivity}_{RO2}[RO_2]t + 2Bt}} \quad (1)$$

This differentiation of ions with the same nominal masses demonstrates a significant advantage of using the ToF-CIMS to discriminate against the detection of side products (Figure 1). Furthermore, we provide experimental evidence to support the unambiguous identification of $I(CH_3C(O)O_2)^-$ and

https://doi.org/10.1021/acs.jpca.1c03140
J. Phys. Chem. A 2021, 125, 6836−6844

Scheme 1. Reaction Schemes for Ketones Photolyzed in This Study[a]

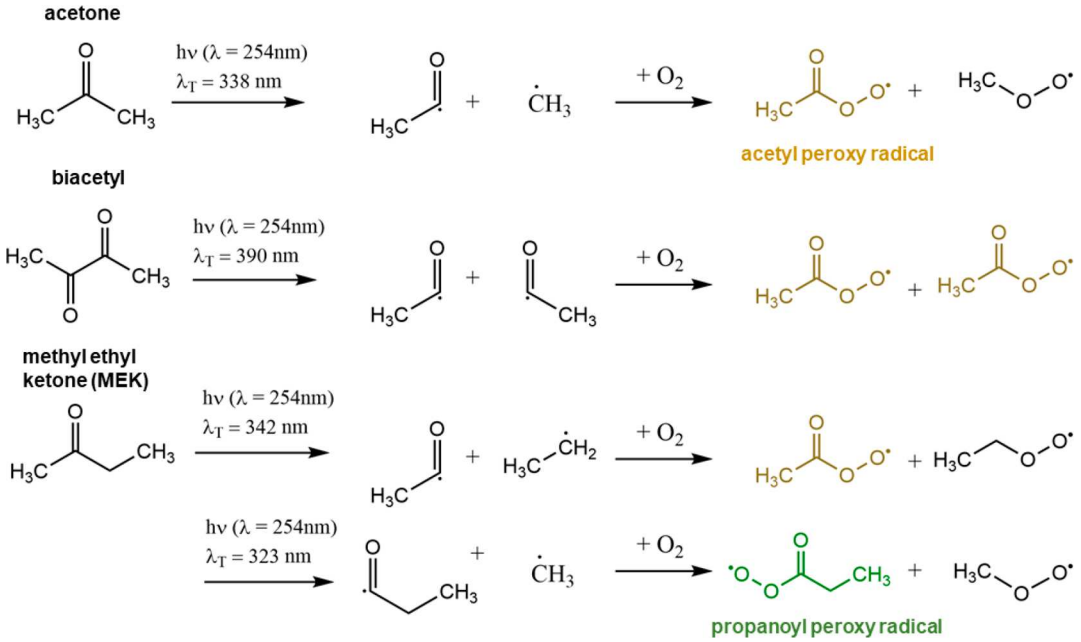

[a]Acetone, biacetyl, and MEK were photolyzed by 254 nm light in the presence of oxygen to form a suite of $RC(O)O_2$ radicals. We highlight the detection and quantification of the acetyl peroxy radical (yellow; $CH_3C(O)O_2$), produced from photolysis of all the ketones, and the propanoyl peroxy radical (green; $CH_3CH_2C(O)O_2$) produced exclusively from the photolysis of MEK. Threshold photolysis wavelengths (λ_T) are calculated from standard enthalpies of formation at 298 K. For simplicity we show only reactions that lead to the production of $RC(O)O_2$ radicals that we can detect. We do not detect other photolysis products (such as CO, C_2H_6, and CH_3 radical).

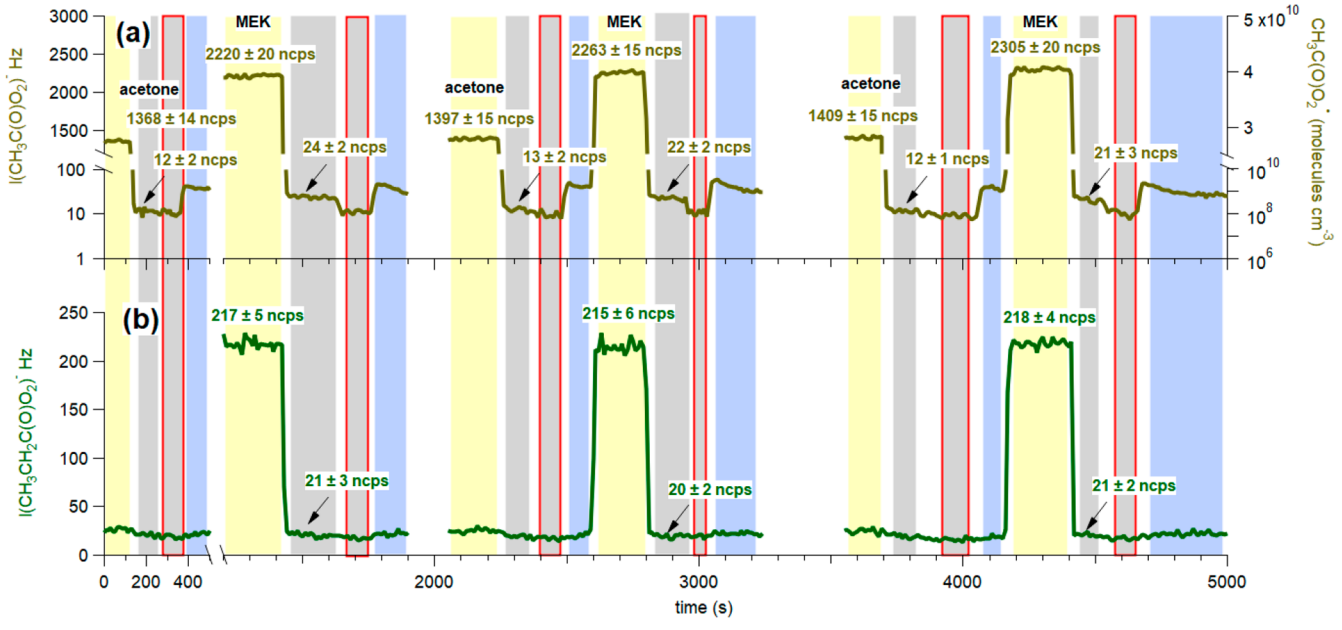

Figure 4. A time series of $R(CO)O_2$ produced from an experiment, performed at a pressure of 865 mbar, alternating the photolysis of acetone (17.7 ppm_v) and MEK (36.1 ppm_v). $CH_3C(O)O_2$ is produced from photolysis of both ketones (panel a; amber trace). $CH_3CH_2C(O)O_2$ (panel b; green trace) is produced exclusively from the photolysis of MEK. The vertical axes of the top panel are discontinuous. The lower portion of the vertical axis is displayed on a logarithmic scale to show the near constancy and low values of the background signals. The colored panels show the signal under the following conditions: gray, light was off with ketones; gray with red border, light off without ketones; yellow, light on with ketones; blue, light on with only bath gas. In these experiments, quantum yields are calculated from the background-subtracted $I(CH_3C(O)O_2)^-$ signals, i.e., signal when ketone is flowing through the reactor with light on (yellow shaded region) minus the signal with light off (gray shaded region). This sequence is repeated with biacetyl or MEK. The shaded regions showing "bath gas and light off" (gray with red boarder) and "bath gas and light on" (blue) demonstrate small background signals of $RC(O)O_2$ that are not photolytically produced. We observe low contributions from all backgrounds (i.e., <3%) to the total signal measured for either $I(CH_3C(O)O_2)^-$ or $I(CH_3CH_2C(O)O_2)^-$.

https://doi.org/10.1021/acs.jpca.1c03140
J. Phys. Chem. A 2021, 125, 6836−6844

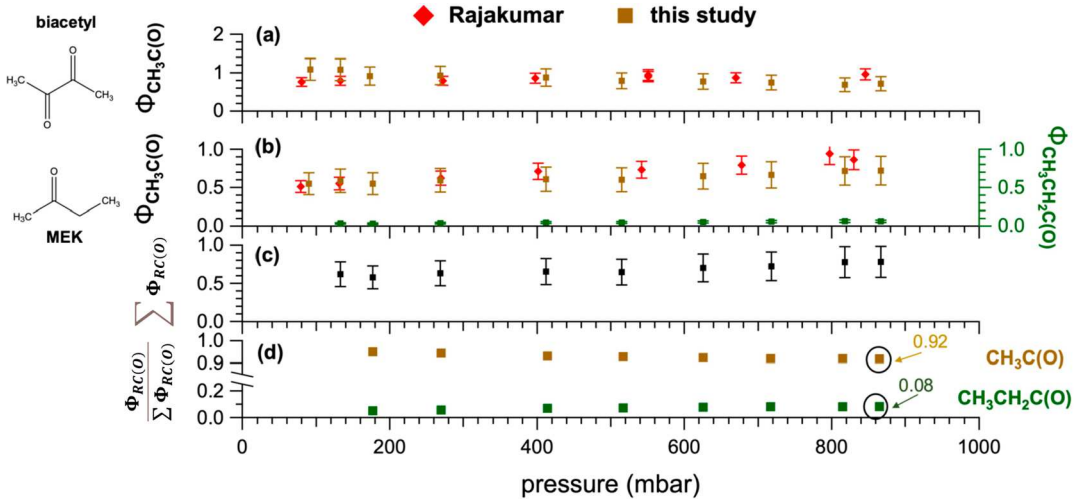

Figure 5. A plot of the measured quantum yields of $CH_3C(O)$ ($\phi_{CH3C(O)}$) as a function of pressure (yellow trace) and compared to the results of Rajakumar et al. (red trace) from photolysis of biacetyl (panel a) and MEK (panels b–d). Markers indicate single measurements (for Rajakumar data) or averages of our five measurements. Error bars for this study represent propagated uncertainty (see Tables 1 and 2 for the measurement precision) of ±26% and include the quoted uncertainties in reported quantum yields by Rajakumar of ±20%. The data are listed in Table 1. The precision of our data is much better than the overall errors shown above. MEK photolysis produces two distinct radicals (panel b), and the quantum yield of $CH_3C(O)$ (amber) is approximately an order of magnitude greater than the quantum yield of $CH_3CH_2C(O)$ (green). The sum of the quantum yields of RC(O) ($\phi_{\sum RC(O)}$) produced from the two photodissociation channels of MEK increase with pressure (panel c). Measurement of both $RC(O)O_2$ simultaneously during the experiment enables quantification of the branching ratio ($\phi_{RC(O)}/\phi_{\sum RC(O)}$) for the MEK photolysis reaction channels (panel d), showing that MEK preferentially produces $CH_3C(O)$ (>90% yield) at 254 nm.

$I(CH_3CH_2C(O)O_2)^-$ ions as $RC(O)O_2$ by reacting the radicals with NO (Figure S3). We note that the absolute concentration of the $RC(O)O_2$ is not needed for calculating the quantum yields that are measured relative to that from acetone. However, quantification is needed to show the suitability of CIMS to measure quantum yields of products with very small concentrations.

MEASUREMENT OF KETONE PHOTOLYSIS QUANTUM YIELDS

We used the above-described experimental system to investigate the photolysis of three ketones: acetone, biacetyl, and MEK. When photolyzed in the presence of oxygen, all three ketones in this study produce $CH_3C(O)O_2$ (Scheme 1).

Figure 4 shows the sequence of steps used to measure the quantum yields. In each experiment, at a given pressure, a known concentration of acetone was flowed through the reactor and photolyzed to produce a stable signal of $I(CH_3C(O)O_2)^-$. Subsequently, acetone was replaced by a known concentration of MEK or biacetyl, and the measurements were repeated. These "back-to-back" experiments allow us to calculate the ratios of the quantum yields of the acyl radical of interest from ketones at 254 nm.

We calculate $CH_3C(O)$ quantum yields ($\phi_{CH3C(O)}$) from biacetyl and MEK using the reported $CH_3C(O)$ quantum yield in the photolysis of acetone at 248 nm by Rajakumar et al. (2009) and the measured ratio of signals. We use Rajakumar et al. (2009) values because they are the only published quantum yield for $CH_3C(O)$ where the radical was detected directly. Using the quantum yield of $CH_3C(O)$ (the precursor for $CH_3C(O)O_2$ formed before its reaction with O_2) from acetone photolysis reported by Rajakumar (2009) as a reference and assuming this is equivalent to the $CH_3C(O)O_2$ quantum yield in our system, the concentration of $CH_3C(O)O_2$ produced from acetone photolysis is

$$[CH_3C(O)O_2] = [CH_3C(O)]_{initial} = \frac{S_{I(CH3C(O)O2)-}}{Sens_{I(CH3C(O)O2)-}} = [acetone] \times \sigma^{acetone}_{254nm} \times \phi^{acetone}_{CH3C(O),248nm}(P) \times F \quad (2)$$

where $S_{I(CH3C(O)O2)-}$ is the $CH_3C(O)O_2$ ToF-CIMS signal (Hz), $Sens_{I(CH3C(O)O2)-}$ is the sensitivity of $CH_3C(O)O_2$ (Hz ppb_v^{-1}), $\sigma^{acetone}_{254nm}$ is the absorption cross-section of acetone at 254 nm (3.01×10^{-20} cm^2 $molecule^{-1}$, 298 K),[5] $\phi^{acetone}_{CH3C(O),248nm}(P)$ is the pressure-dependent quantum yield reported in Rajakumar (2009) for $CH_3C(O)$, and F is the 254 nm photon flux from the lamp (photons cm^{-2} s^{-1}) in the reactor. When comparing equivalent reaction times, the $\phi_{CH3C(O)}$ from biacetyl and MEK photolysis can be determined by comparing the amount of $CH_3C(O)O_2$ production from acetone with biacetyl and MEK (shown as "ketone" in eq 3) through the equation

$$\phi^{ketone}_{CH3C(O),254nm}(P) = \frac{S^{ketone}_{I(CH3C(O)O2)-} \times [acetone] \times \sigma^{acetone}_{254nm} \times \phi^{acetone}_{CH3C(O),248nm}(P)}{S^{acetone}_{I(CH3C(O)O2)-} \times [ketone] \times \sigma^{ketone}_{254nm}} \quad (3)$$

In the absence of a reliable calibration source, we assumed that $CH_3CH_2C(O)O_2$ has a detection sensitivity identical to that of $CH_3C(O)O_2$ and use eq 3 to calculate quantum yields for $CH_3CH_2C(O)$ from MEK photolysis. We discuss the justification for this assumption in the Supporting Information. Also, note that the ratio of the signal levels for $CH_3C(O)O_2$ and $CH_3CH_2C(O)O_2$ in MEK photolysis yields the ratio of the quantum yields for $CH_3C(O)$ and $CH_3CH_2C(O)$ as long as our assumption of the equal detection sensitivity is valid.

Figure 5 shows the $\phi_{CH3C(O)}$, as a function of pressure, determined in this study compared to those by Rajakumar et al.

https://doi.org/10.1021/acs.jpca.1c03140
J. Phys. Chem. A 2021, 125, 6836–6844

The measured quantum yields, along with the experimental conditions employed to measure them, are shown in Tables 1 and 2 for biacetyl and MEK photolyses.

Table 1. Measured Quantum Yields in the Photolysis of Biacetyl as a Function of Pressure of Air[a]

pressure (mbar)	[biacetyl] (ppm_v, range)	[acetone] (ppm_v, range)	biacetyl $\Phi_{CH3C(O)}$ (avg ± 2σ)
92	5−68	8−62	1.09 ± 0.25
133	28−64	14−23	1.08 ± 0.28
173	28−71	16−34	0.92 ± 0.12
269	8−59	9−31	0.93 ± 0.10
412	12−40	7−21	0.88 ± 0.06
515	13−31	8−16	0.79 ± 0.06
626	9−31	8−16	0.77 ± 0.08
718	4−32	7−20	0.74 ± 0.13
818	3−30	6−17	0.69 ± 0.05
867	9−27	13−18	0.71 ± 0.09

[a]A minimum of five measurements were done at 303 ± 3 K. Experimental uncertainty is ±26% including the estimated systematic errors due to the uncertainties quoted by Rajakumar et al. for the quantum yields of $CH_3C(O)$ in the photolysis of acetone. The quoted uncertainty is the precision of the measurements.

We observe the $\phi_{CH3C(O)}$ from biacetyl to decrease slightly when going from low to high pressures as one would expect from quenching of the initial excited state. In contrast to biacetyl, the $\phi_{CH3C(O)}$ from MEK photolysis increases from ∼0.52 to 0.72 between 90 and 865 mbar. This result is qualitatively similar to the results of Rajakumar et al. obtained by an entirely different method. This increase in quantum yield with pressure is consistent with the stabilization of the photolytically produced excited RC(O) radical by the bath gas; such a behavior has also been reported for 248 nm photolysis by Khamaganov et al.[4] There are some small quantitative differences at pressures above 200 mbar, but they are within the experimental uncertainties.

The $\phi_{CH3C(O)}$ values from biacetyl and MEK determined from this study are slightly higher at pressures below 200 mbar than the corresponding $\phi_{CH3C(O)}$ determined by Rajakumar. The possible reasons for the observed deviations from the results of Rajakumar include the following: (1) we used a Pen-Ray lamp which had emissions not only at 254 nm but also at 316 and 365 nm (Figure 2 and Table S1); (2) we used air ($[O_2] \approx 21\%$) while Rajakumar et al. used N_2; (3) the reference values of $\phi_{CH3C(O)}$ from acetone photolysis occur within the region where the quantum yield falls off rapidly at lower pressures. Overall, we suggest that the general close agreement in $\phi_{CH3C(O)}$ determined in this study to those determined by Rajakumar using a visible absorption method provides evidence that our ToF-CIMS method is a robust way to measure photodissociation product quantum yields.

Assuming the detection sensitivities for $CH_3CH_2(O)O_2$ and $CH_3C(O)O_2$ are the same, we calculate a $\phi_{CH3CH2C(O)}$ that ranges from ∼0.03 to 0.07 between 177 and 865 mbar. Because the quantum yields determined from the measurement of the two $RC(O)O_2$ represent two distinct photolysis channels for MEK, we suggest that the sum of the quantum yields from these two channels is a lower bound on the total quantum yield for MEK photodissociation (Figure 5c). We estimate a lower-bound for the MEK photolysis (at 254 nm) quantum yield at 865 mbar to be 0.77. The branching ratio for the two acyl radicals in the MEK photolysis is nearly constant across the range of pressures tested (92% to $CH_3C(O)$ and 8% to $CH_3CH_2C(O)$). This finding is consistent with a previous measurement at 275 nm,[23] which suggested that MEK photolysis yields mainly $CH_3C(O)$. Additionally, our results show remarkable agreement with the recent observations of photolysis branching ratios in the photolysis of MEK at 285 nm from Zborowska et al.[24] suggesting that the branching value for $CH_3C(O)$ of 0.93 is also independent of pressure above 250 mbar.

Effect of Secondary Reactions on Quantum Yields. Secondary reactions (including peroxy radical self-reactions) can change the measured quantum yield of RO_2 from photolysis experiments. We evaluated the susceptibility of our experimental design to the measured quantum yields due to secondary loss (or production) of the detected products.

Upon decreasing the reaction time (which includes the time for transfer of the effluents to the CIMS) from 1.5 to 0.32 s, we observe an increase in the quantum yield of both RC(O) (R is either CH_3 or C_2H_5) of <15%. These experiments were performed at 865 mbar. It is important to note that we generate the photolysis radicals over a 5 cm region where the flow rate is >3 times faster than in the rest of the flow reactor. We plot the inverse of the RC(O) quantum yield as a function of reaction time to determine the approximate second order

Table 2. Measured Quantum Yields in the Photolysis of MEK as a Function of Air Pressure[a]

pressure (mbar)	[MEK] (ppm_v, range)	[acetone] (ppm_v, range)	MEK $\Phi_{CH3C(O)}$ (avg ± 2σ)	MEK $\Phi_{CH3CH2C(O)}$ (avg ± 2σ)	MEK $\sum\Phi_{RC(O)}$ (avg ± 2σ)	MEK $CH_3C(O)$ branching ratio[b]
90	75−92	16−21	0.55 ± 0.05			
133	82−99	24−29	0.59 ± 0.03	0.034 ± 0.011	0.62 ± 0.03	0.95
177	85−105	25−30	0.55 ± 0.01	0.030 ± 0.006	0.58 ± 0.01	0.95
269	71−83	29−35	0.59 ± 0.03	0.038 ± 0.004	0.63 ± 0.03	0.94
412	44−56	19−24	0.61 ± 0.07	0.047 ± 0.008	0.66 ± 0.07	0.93
515	36−45	16−19	0.60 ± 0.04	0.047 ± 0.004	0.65 ± 0.04	0.93
626	34−41	16−19	0.65 ± 0.02	0.054 ± 0.002	0.70 ± 0.02	0.92
718	37−47	18−22	0.66 ± 0.04	0.058 ± 0.004	0.72 ± 0.04	0.92
818	33−42	16−20	0.71 ± 0.05	0.063 ± 0.005	0.77 ± 0.05	0.92
867	34−36	16−18	0.72 ± 0.05	0.063 ± 0.007	0.78 ± 0.05	0.92

[a]A minimum of five measurements were done at 303 ± 3 K. Experimental uncertainty is ±26% including the estimated systematic errors due to the uncertainties quoted by Rajakumar et al. for the quantum yields of $CH_3C(O)$ in the photolysis of acetone. [b]We do not quote uncertainties in the branching ratios since we assume the detection efficiencies for $I(CH_3CO(O)_2)^-$ and $I(C_2H_5C(O)O_2)^-$ to be the same. These are ratios of the quantum yields for the two channels.

https://doi.org/10.1021/acs.jpca.1c03140
J. Phys. Chem. A 2021, 125, 6836−6844

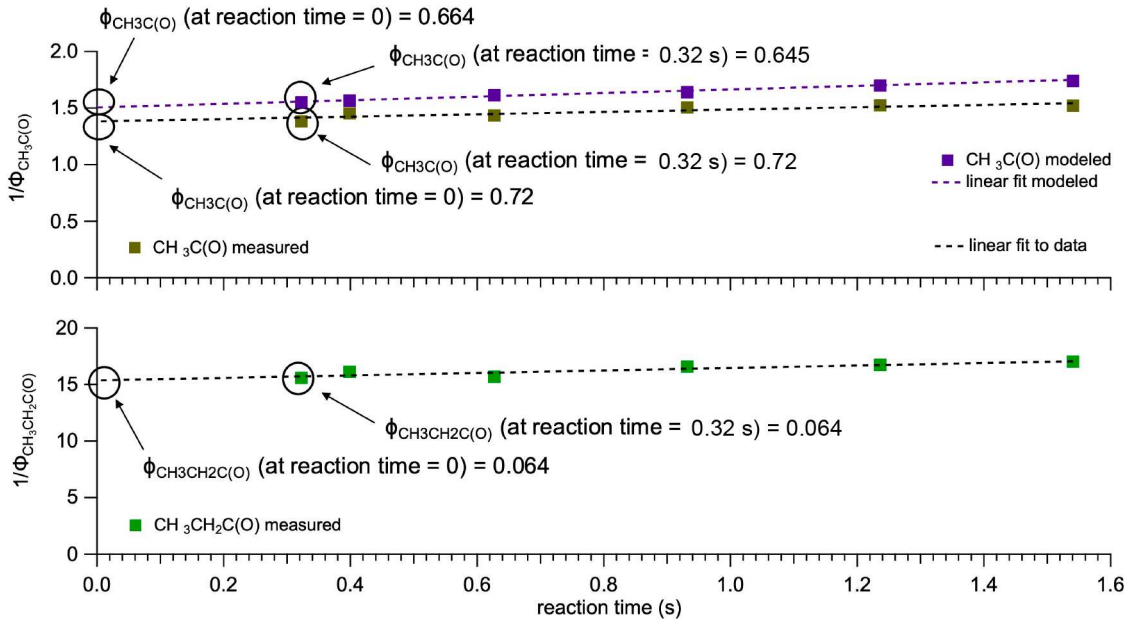

Figure 6. Inverse quantum yields are plotted as a function of reaction time to determine the effect of secondary reactions. Modeled values (purple) were determined using starting concentrations of $CH_3C(O)O_2$ for acetone ($[CH_3C(O)O_2]$ = 301 pptv) and modeled for five different reaction times. The $\phi_{CH3C(O)}$ determined from the *y*-intercept of an analysis assuming a second-order loss for the peroxy radicals is within 3% of the $\phi_{CH3C(O)}$ calculated at the reaction time represented in this study (0.32 s).

rate constant for the loss of $RC(O)O_2$ and $RC(O)$ and to estimate the quantum yields at a reaction time of zero. The results of a linear regression, in the context of second order kinetics, show that for both $CH_3C(O)$ and $C_2H_5C(O)$ radicals the "initial" quantum yields (i.e., reaction time = 0 s) are essentially identical to the quantum yields measured at short reaction times (Figure 6). The loss rate of the $RC(O)O_2$ radical is complicated because the photolysis region is not negligible, and we generate CH_3O_2 in addition to $CH_3C(O)O_2$. However, by accounting for these reactions, we calculate a rough rate constant for the self-reaction of $CH_3C(O)O_2$ radical to be 9.5×10^{-12} cm^3 $molecule^{-1}$ s^{-1}, which is consistent with the known rate coefficients for the reactions of $CH_3C(O)O_2$ with itself and CH_3O_2.[25] This analysis supports the conclusion that we have optimized the reaction time in our system to decrease the influence of secondary reactions. In the future, use of very short photolysis volume (e.g., using a laser) would allow us to control the reaction time more precisely.

We also used a box model to determine the effects of $RC(O)O_2$ + $RC(O)O_2$, $RC(O)O_2$ + RO_2, and $RC(O)O_2$ + HO_2 reactions on the $CH_3C(O)O_2$ observed in this study; the reactions used for this model are shown in the Supporting Information (Table S3). We determine that secondary reactions likely decrease our measured $\phi_{CH3C(O)}$ by at most 3% (Figure 6). Unfortunately, with I^- reagent ion, we could not measure the yield of CH_3 from the photodissociation of acetone or MEK due to an interference at that unit mass. The use of other reagent ions would overcome this problem, and such experiments are planned.

■ ADVANTAGES AND APPLICATIONS OF CIMS FOR QUANTUM YIELD MEASUREMENTS

From our experiments described here, we suggest that several qualities of ToF-CIMS make it a viable tool for quantifying photodissociation product quantum yields:

- ToF-CIMS is a highly sensitive technique for measuring $RC(O)O_2$ (i.e., LOD = 6 ppt_v for $CH_3C(O)O_2$; this sensitivity can be enhanced by signal averaging longer). Therefore, one could utilize light sources that are not very intense.
- The selectivity of the reagent ion (in this case, iodide ion) allows for low background and interference from unwanted impurities or reaction products, as demonstrated by low background signals in our photolysis experiments.
- Multiple similar radicals can be measured simultaneously, which allows a more straightforward determination of branching ratios and total photodissociation quantum yields. Evaluating the possible differences in the detection sensitivities would enhance this method.

In addition to highlighting the advantages of ToF-CIMS in this current laboratory-based application, we note some of the potential future applications:

- Replacing the UV pen-lamp used in this study with a light source capable of producing wavelengths relevant for ketone photolysis (<400 nm) would help quantify important knowledge gaps in photolysis quantum yields.
- This experimental design could measure atmospheric ketone photolysis under a field setting because of the portability of the instrument.
- Rapid data acquisition (<1 Hz) of $RC(O)O_2$ signals allows for in situ observations of photolysis processes in ambient environments.[26]
- Use of a light source where the photolysis volume is small allows for better control of reaction times and simultaneous measurements of the kinetics of the radicals involved.
- Equipping the mass spectrometer with reagent-switching capabilities[27,28] would allow for measurement of multiple photolysis products[29] and the photolytic loss of carbonyl photolyte.[30]

https://doi.org/10.1021/acs.jpca.1c03140
J. Phys. Chem. A 2021, 125, 6836−6844

■ ASSOCIATED CONTENT

Supporting Information

The Supporting Information is available free of charge at https://pubs.acs.org/doi/10.1021/acs.jpca.1c03140.

Additional information on the PAN calibration source, CIMS characterization of RO_2, experimental design tests, and measurement artifacts (PDF)

■ AUTHOR INFORMATION

Corresponding Authors

Michael F. Link − *Department of Chemistry, Colorado State University, Fort Collins, Colorado 80523, United States;* orcid.org/0000-0002-1841-2455; Email: linkmf@rams.colostate.edu

A. R. Ravishankara − *Department of Chemistry and Department of Atmospheric Science, Colorado State University, Fort Collins, Colorado 80523, United States;* orcid.org/0000-0001-9059-8437; Email: A.R.Ravishankara@colostate.edu

Authors

Delphine K. Farmer − *Department of Chemistry, Colorado State University, Fort Collins, Colorado 80523, United States;* orcid.org/0000-0002-6470-9970

Tyson Berg − *Department of Chemistry, Colorado State University, Fort Collins, Colorado 80523, United States*

Frank Flocke − *National Center for Atmospheric Research, Boulder, Colorado 80301, United States*

Complete contact information is available at: https://pubs.acs.org/10.1021/acs.jpca.1c03140

Notes

The authors declare no competing financial interest.

■ ACKNOWLEDGMENTS

We thank NSF for funding (Grant 1922619).

■ REFERENCES

(1) Somnitz, H.; Fida, M.; Ufer, T.; Zellner, R. Pressure Dependence for the CO Quantum Yield in the Photolysis of Acetone at 248 nm: A Combined Experimental and Theoretical Study. *Phys. Chem. Chem. Phys.* **2005**, *7* (18), 3342.

(2) Somnitz, H.; Ufer, T.; Zellner, R. Acetone Photolysis at 248 Nm Revisited: Pressure Dependence of the CO and CO_2 Quantum Yields. *Phys. Chem. Chem. Phys.* **2009**, *11* (38), 8522−8531.

(3) Emrich, M.; Warneck, P. Photodissociation of Acetone in Air: Dependence on Pressure and Wavelength. Behavior of the Excited Singlet State. *J. Phys. Chem. A* **2000**, *104* (42), 9436−9442.

(4) Khamaganov, V.; Karunanandan, R.; Rodriguez, A.; Crowley, J. N. Photolysis of CH3C(O)CH3 (248 nm, 266 nm), CH3C(O)C2H5 (248 nm) and CH3C(O)Br (248 nm): Pressure Dependent Quantum Yields of CH3 Formation. *Phys. Chem. Chem. Phys.* **2007**, *9* (31), 4098−4113.

(5) Gierczak, T.; Burkholder, J. B.; Bauerle, S.; Ravishankara, A. R. Photochemistry of Acetone under Tropospheric Conditions. *Chem. Phys.* **1998**, *231* (2), 229−244.

(6) Blitz, M. A.; Heard, D. E.; Pilling, M. J. Study of Acetone Photodissociation over the Wavelength Range 248−330 Nm: Evidence of a Mechanism Involving Both the Singlet and Triplet Excited States. *J. Phys. Chem. A* **2006**, *110* (21), 6742−6756.

(7) Brewer, J. F.; Bishop, M.; Kelp, M.; Keller, C. A.; Ravishankara, A. R.; Fischer, E. V. A Sensitivity Analysis of Key Natural Factors in the Modeled Global Acetone Budget. *J. Geophys. Res.: Atmos.* **2017**, *122* (3), 2043−2058.

(8) Arnold, F.; Bürger, V.; Droste-Franke, B.; Grimm, F.; Krieger, A.; Schneider, J.; Stilp, T. Acetone in the Upper Troposphere and Lower Stratosphere: Impact on Trace Gases and Aerosols. *Geophys. Res. Lett.* **1997**, *24* (23), 3017−3020.

(9) Neumaier, M.; Ruhnke, R.; Kirner, O.; Ziereis, H.; Stratmann, G.; Brenninkmeijer, C. A. M.; Zahn, A. Impact of Acetone (Photo)Oxidation on HOx Production in the UT/LMS Based on CARIBIC Passenger Aircraft Observations and EMAC Simulations. *Geophys. Res. Lett.* **2014**, *41* (9), 3289−3297.

(10) Fischer, E. V.; Jacob, D. J.; Yantosca, R. M.; Sulprizio, M. P.; Millet, D. B.; Mao, J.; Paulot, F.; Singh, H. B.; Roiger, A.; Ries, L.; Talbot, R. W.; Dzepina, K.; Deolal, S. P. Atmospheric Peroxyacetyl Nitrate (PAN): A Global Budget and Source Attribution. *Atmos. Chem. Phys.* **2014**, *14* (5), 2679−2698.

(11) Burkholder, J. B.; Sander, S. P.; Abbatt, J. P. D.; Barker, J. R.; Cappa, C.; Crounse, J. D.; Dibble, T. S.; Huie, R. E.; Kolb, C. E.; Kurylo, M. J.; Orkin, V. L.; Percival, C. J.; Wilmouth, D. M.; Wine, P. H. *Chemical Kinetics and Photochemical Data for Use in Atmospheric Studies; Evaluation Number 19*; Technical Report; Jet Propulsion Laboratory, National Aeronautics and Space Administration: Pasadena, CA, 2020.

(12) Meyrahn, H.; Pauly, J.; Schneider, W.; Warneck, P. Quantum Yields for the Photodissociation of Acetone in Air and an Estimate for the Life Time of Acetone in the Lower Troposphere. *J. Atmos. Chem.* **1986**, *4* (2), 277−291.

(13) Khamaganov, V. G.; Crowley, J. N. Pressure Dependent Photolysis Quantum Yields for CH3C(O)CH3 at 300 and 308 nm and at 298 and 228 K. *Phys. Chem. Chem. Phys.* **2013**, *15* (25), 10500−10509.

(14) Haas, Y. Photochemical α-Cleavage of Ketones: Revisiting Acetone. *Photochem. Photobiol. Sci.* **2004**, *3* (1), 6−16.

(15) Blitz, M. A.; Heard, D. E.; Pilling, M. J.; Arnold, S. R.; Chipperfield, M. P. Pressure and Temperature-Dependent Quantum Yields for the Photodissociation of Acetone between 279 and 327.5 nm. *Geophys. Res. Lett.* **2004**, *31* (6), L06111.

(16) Rajakumar, B.; Gierczak, T.; Flad, J. E.; Ravishankara, A. R.; Burkholder, J. B. The CH3CO Quantum Yield in the 248nm Photolysis of Acetone, Methyl Ethyl Ketone, and Biacetyl. *J. Photochem. Photobiol., A* **2008**, *199* (2), 336−344.

(17) Bertram, T. H.; Kimmel, J. R.; Crisp, T. A.; Ryder, O. S.; Yatavelli, R. L. N.; Thornton, J. A.; Cubison, M. J.; Gonin, M.; Worsnop, D. R. A Field-Deployable, Chemical Ionization Time-of-Flight Mass Spectrometer. *Atmos. Meas. Tech.* **2011**, *4* (7), 1471−1479.

(18) Lee, B. H.; Lopez-Hilfiker, F. D.; Mohr, C.; Kurtén, T.; Worsnop, D. R.; Thornton, J. A. An Iodide-Adduct High-Resolution Time-of-Flight Chemical-Ionization Mass Spectrometer: Application to Atmospheric Inorganic and Organic Compounds. *Environ. Sci. Technol.* **2014**, *48* (11), 6309−6317.

(19) Lopez-Hilfiker, F. D.; Iyer, S.; Mohr, C.; Lee, B. H.; D'Ambro, E. L.; Kurtén, T.; Thornton, J. A. Constraining the Sensitivity of Iodide Adduct Chemical Ionization Mass Spectrometry to Multifunctional Organic Molecules Using the Collision Limit and Thermodynamic Stability of Iodide Ion Adducts. *Atmos. Meas. Tech.* **2016**, *9* (4), 1505−1512.

(20) Iyer, S.; He, X.; Hyttinen, N.; Kurtén, T.; Rissanen, M. P. Computational and Experimental Investigation of the Detection of HO_2 Radical and the Products of Its Reaction with Cyclohexene Ozonolysis Derived RO_2 Radicals by an Iodide-Based Chemical Ionization Mass Spectrometer. *J. Phys. Chem. A* **2017**, *121* (36), 6778−6789.

(21) Atkinson, R.; Baulch, D. L.; Cox, R. A.; Crowley, J. N.; Hampson, R. F.; Hynes, R. G.; Jenkin, M. E.; Rossi, M. J.; Troe, J.; IUPAC Subcommittee.. Evaluated Kinetic and Photochemical Data for Atmospheric Chemistry: Volume II − Gas Phase Reactions of Organic Species. *Atmos. Chem. Phys.* **2006**, *6* (11), 3625−4055.

(22) Flocke, F. M.; Weinheimer, A. J.; Swanson, A. L.; Roberts, J. M.; Schmitt, R.; Shertz, S. On the Measurement of PANs by Gas

Chromatography and Electron Capture Detection. *J. Atmos. Chem.* **2005**, *52* (1), 19−43.
(23) Raber, W. H.; Moortgat, G. K. Photooxidation of Selected Carbonyl Compounds in Air: Methyl Ethyl Ketone, Methyl Vinyl Ketone, Mathacrolein, and Methylglyoxal. *Progress and problems in atmospheric chemistry* **1995**, *3*, 318.
(24) Zborowska, A. G.; MacInnis, C. Y.; Ye, C. Z.; Osthoff, H. D. On the Photolysis Branching Ratio of Methyl Ethyl Ketone. *Atmos. Environ.* **2021**, *254*, 118383.
(25) Tyndall, G. S.; Cox, R. A.; Granier, C.; Lesclaux, R.; Moortgat, G. K.; Pilling, M. J.; Ravishankara, A. R.; Wallington, T. J. Atmospheric Chemistry of Small Organic Peroxy Radicals. *Journal of Geophysical Research: Atmospheres* **2001**, *106* (D11), 12157−12182.
(26) Eger, P. G.; Schuladen, J.; Sobanski, N.; Fischer, H.; Karu, E.; Williams, J.; Vakkari, V.; Lelieveld, J.; Crowley, J. N. Modelling the Impact of Gas-Phase Pyruvic Acid on Acetaldehyde and Peroxy Radical Formation in the Boreal Forest. *Atmos. Chem. Phys. Discuss.* **2020**, 1−27.
(27) Brophy, P.; Farmer, D. K. A Switchable Reagent Ion High Resolution Time-of-Flight Chemical Ionization Mass Spectrometer for Real-Time Measurement of Gas Phase Oxidized Species: Characterization from the 2013 Southern Oxidant and Aerosol Study. *Atmos. Meas. Tech.* **2015**, *8* (7), 2945−2959.
(28) Rissanen, M. P.; Mikkilä, J.; Iyer, S.; Hakala, J. Multi-Scheme Chemical Ionization Inlet (MION) for Fast Switching of Reagent Ion Chemistry in Atmospheric Pressure Chemical Ionization Mass Spectrometry (CIMS) Applications. *Atmos. Meas. Tech.* **2019**, *12* (12), 6635−6646.
(29) Sanchez, J.; Tanner, D. J.; Chen, D.; Huey, L. G.; Ng, N. L. A New Technique for the Direct Detection of HO_2 Radicals Using Bromide Chemical Ionization Mass Spectrometry (Br-CIMS): Initial Characterization. *Atmos. Meas. Tech.* **2016**, *9* (8), 3851−3861.
(30) Koss, A. R.; Warneke, C.; Yuan, B.; Coggon, M. M.; Veres, P. R.; de Gouw, J. A. Evaluation of NO^+ Reagent Ion Chemistry for Online Measurements of Atmospheric Volatile Organic Compounds. *Atmos. Meas. Tech.* **2016**, *9* (7), 2909−2925.

https://doi.org/10.1021/acs.jpca.1c03140
J. Phys. Chem. A 2021, 125, 6836−6844